ATLANTIS PRESS
Advances in Engineering Research, volume 94
2nd International Conference on Sustainable Development (ICSD 2016)

Synthesis and Characterization of Surface Ion-imprinted Polymer Based on Mesoporous Silica SBA-15 for Selective Removal of Cu(II) from Aqueous Solutions

Sheng-fang LI[1], Lin YANG[1], Wei-jun SONG[1] and Chun-yan SUN[1,*]
[1]Department of Chemical Engineering, Qinghai University,Xining, China.
Corresponding Author*e-mail: sunchunyan@qhu.edu.cn
e-mail: 1620449624@qq.com

***Abstract*—A Cu(II) ion-imprinted polymer (Cu(II)-IIP) for the selective adsorption and separation of Cu(II) was prepared by modifying the surface of mesoporous silica SBA-15 through surface ion imprinting. The prepared polymer was characterized by Fourier transmission infrared spectra (FT-IR), X-ray diffraction (XRD), Energy disperse spectrometer (EDS), Thermogravimetric analysis(TGA), Scanning electron microscope (SEM), Transmission electron microscope (TEM) and nitrogen adsorption–desorption isotherm. Batch adsorption tests were investigated on the effects of solution pH value, contact time and different initial Cu(II) ion concentrations. The results showed that the Cu(II)-IIP has higher adsorption capacity and selectivity than that of non-imprinted polymer (NIP). The adsorption isotherm followed Langmuir model. The kinetic data well fitted the pseudo-second-order kinetic model compared with the pseudo-first-order kinetic model. The selectivity coefficients for Cu(II)/Cd(II), Cu(II)/Fe(II), Cu(II)/Co(II), Cu(II)/Pb(II) were 3.56, 2.32, 11.75, 4.73, respectively. In addition, Adsorption capacity did not significantly decrease after five adsorption–desorption cycles were completed. demonstrating that the polymer is stable and reusable.**

Keywords-Ion-imprinted polymer; Mesoporous silica ; Surface imprinting technology; Cu(II) ; Adsorption

I. INTRODUCTION

Copper is an essential trace element for our health, but excessive amount of copper in human body can cause serious damage, even it can be toxic at the concentrations as low as 1 $\mu g \cdot L^{-1}$ [1,2]. Nowadays water pollution by heavy metals has become a worldwide environmental problem because of their toxicity towards aquatic-life, human beings and environment [3-5]. Thus, effective removal and determination of trace amounts of copper in the environmental or biological samples is essential.

To date, numerous technologies have been developed for heavy metals removal from wastewater, such as electrodialysis, chemical precipitation, ion exchange, adsorption and membrane filtration [6-8]. Among them, adsorption plays an important role due to its flexibility in design, operation and superior efficiency under certain conditions [9]. Conventional absorbents, like activated carbon, zeolites, clays and metal oxides [10-13], have some disadvantages for the removal of heavy metals. Such as non-specific, low selectivity, poor hydrothermal stability and low reusability [14]. On the other hand, various detection techniques has also been developed, including inductively coupled plasma optical emission spectrometry (ICP-OES), inductively coupled plasma mass spectrometry (ICP-MS) and atomic absorption spectrometry (AAS) [15,16]. AAS, nowadays is still one of the most frequently used analytical techniques for the metals determination. However, its relatively low sensitivity and performances in complex matrices seriously impact on its further applications in trace analysis [17]. Therefore, it is necessary to develop a highly selective sorbent for preconcentration and determination of Cu(II) ions in solutions.

Ion imprinting is a type of molecular imprinting technique with remarkable recognition properties because of their template ions [18]. Ion imprinting polymer (IIP) obtained by traditional methods may lead to the poor site accessibility to the target ions, slow mass-transfer rate and incomplete removal of templates, while a burgeoning method, surface imprinting [19,20], to some extent, can solve the above problems.

The advances in this field have found that the support materials usually used include magnetic materials [21], carbon-based materials [22], silicon-based materials [23] and so on. Among mesoporous silicon family, SBA-15 is an attractive candidate to be used as a support for surface ion imprinting polymer due to its large surface area, highly ordered pore, thick pore walls with high hydrothermal stability and available surface functionalization [24,25]. Meng et al. [26] prepared cesium ion-imprinted polymer based on SBA-15 by RAFT polymerization strategies, the polymer exhibited more homogeneous and thin polymer layer with higher adsorption property than the polymer prepared using the free RAFT agent in solution . Liu et al. [27] Tailor-made ion-imprinted polymer based on functionalized graphene oxide for the preconcentration and determination of trace copper in food samples. which achieve the excellent combination of support materials and surface imprinting technique.

In the study, Cu(II)-IIP supported on SBA-15 was easily prepared with low cost via surface imprinting technique. The structural characteristics, adsorption behavior of the Cu(II)-IIP towards Cu(II) ions in aqueous solution were tested and discussed in detail.

II. EXPERIMENTAL

A. Materials and Chemicals

Poly(ethyleneglycol)-block-poly(propyleneglycol)-block-poly(ethylene glycol) ($EO_{20}PO_{70}EO_{20}$, molecular weight5800)(P123,Sigma,USA),tetraethylorthosilicate(TEOS),3-(methacryloxyl) propyltrimethoxysilane (MPS, 97%), methyl acrylic acid (MAA, 98%), ethylene glycoldimethacrylate (EGDMA, average Mn 750), 2,2'-azobisisobutyronitrile (AIBN, 99%) were purchased from Aladdin (Shanghai, China). All the other chemicals used were of analytical grade. Doubly distilled water (DDW) was used for all dilutions.

B. Apparatus and Measurements

Fourier-transform infrared (FT-IR) spectra were obtained with a Perkin-Elmer FTIR Spectrum BX-II spectrometer using KBr pellets over the range of 400–4000 cm^{-1} at room temperature. Energy dispersive spectrometry (EDS) was performed with a United Oxford Instruments JSM-5610LV/INCA using to confirm the existence of elements in Cu(II)-IIP. The thermogravimetry (TG) analysis was performed with a NETZSCH STA 449 F3 instrument in owing N_2 with a heating rate of 5 °C/min. Small-angle X-ray diffraction (SAXRD) analysis was carried out using a PANalytic X'Pert PRO MPD diffractometer over the 2θ range of 0.5°–5°, CuKa (40 kV and 20 mA) radiation was used. The step size was 0.008° and the nominal collecting time was 50.16 s per step. Scanning electron microscopy (SEM) was utilized for assessing the morphology of the obtained polymers by using JEOL JSM-6610LV at 25 kV. Transmission electron microscopy (TEM) images were taken using a Tecnai TF20 G2 FEG-TEM at 200 kV accelerating voltage with a standard single-tilt holder. The sample was dispersed into anhydrous alcohol with ultrasonic treatment for 20 min, and the solution was deposited on a Cu grid. Nitrogen adsorption–desorption isotherms were obtained at −197 °C using a 3H-2000PS1 specific surface area and pore size analyzer. Prior to the adsorption experiment, the materials were vacuum dried at 200 °C for 10 h. The specific surface area and pore size distribution of the product were calculated by the BET and BJH methods, respectively. Flame atom absorption spectrometry (FAAS) was used to determination of Cu(II) ions and other metal ions such as Cd(II), Fe(II), Co(II), Pb(II) by using Shimadzu AA-6300C. All the solutions were prepared with ultra-pure water (18.25 MΩ*cm resistivity) obtained from a Milli-Q Direct 16 water purification system.

C. Preparation of Cu(II)-IIP

1) Preparation and activation of SBA-15

SBA-15, as the support matrix, was synthesized according to Zhao et al. [28]. To obtain the activated SBA-15, the prepared SBA-15 was treated with 3 $mol\cdot L^{-1}$ HCl by refluxing for 24 h at 80 °C , followed by washing with DDW to neutral pH. Finally, the product was dried at 60 °C . Then, the activated SBA-15 was obtained.

2) Preparation of SBA-15@MPS

150 mg of activated SBA-15 and 3 mL MPS were dispersed in 40 mL absolute ethanol and stirred under nitrogen at 50 °C for 24 h. The mixture was filtered and the modified SBA-15 (SBA-15@MPS) was rinsed with ethanol several times and dried at 60 °C for 6 h.

3) Preparation of Cu(II)-IIP

1 mmol of $CuCl_2$, 4 mmol of MAA and 0.1 g SBA-15@MPS were dispersed into 30 mL of methanol and 10mL DDW stirred under nitrogen at room temperature for 2 h, after polymerization, 10 mL EGDMA and 10 mg AIBN were added into this suspension. The resultant mixture was stirred by refluxing in a water bath at 65 °C for 6 h under nitrogen protection. Subsequently, the prepared polymer was washed with methanol/water (4:1, v/v) for several times to purify the products. Finally, the adsorbent was treated with 2 $mol\cdot L^{-1}$ HCl to completely leach the non-covalent Cu(II) and dried in vacuum. As a control, non-imprinted polymer was also prepared as a blank in parallel, but without the addition of $CuCl_2$.

D. Adsorption Experiments

1) Static adsorption studies

Adsorption of Cu(II) from aqueous solutions was investigated in batch experiments. 20 mg of Cu(II)-IIP was added into 20 mL of Cu(II) with different concentration in the pH range of 3–8 and the mixture was shaken for 180 min at 25 °C . Afterwards, the mixture solution was centrifuged and the concentration of the residual Cu(II) was measured by FAAS. The absorption capacity q_e , q_t ($mg\cdot g^{-1}$) at equilibrium and time t (min) were calculated as follows:

$$q_e = \frac{(C_0 - C_e)V}{m} \tag{1}$$

$$q_t = \frac{(C_0 - C_t)V}{m} \tag{2}$$

where C_0, C_e and C_t ($mg\cdot L^{-1}$)are concentrations of Cu(II) at initial, equilibrium and time t in aqueous phase, respectively. V (mL) and m (g) are the volume of solution and the mass of the sorbent, respectively.

2) Selectivity study

In order to measure the selectivity of the imprinted polymer, binary binding ability of M(Cd(II), Fe(II), Co(II), Pb(II))metals with respect to Cu(II) was investigated using Cu(II)-IIP and NIP. 20mg of Cu(II)-IIP or NIP was added in 20 mL of 100 $mg\cdot L^{-1}$ binary metal mixed solutions. Finally, The distribution coefficient K_d ($mL\cdot g^{-1}$), selectivity coefficient k, and the relative selectivity coefficient k' [29] were given as follows:

$$K_d = \frac{(C_0 - C_e)V}{mC_e} \tag{3}$$

$$k = \frac{K_d(Cu(\mathrm{II}))}{K_d(M)} \tag{4}$$

$$k' = \frac{k_{IIP}}{k_{NIP}} \quad (5)$$

where K_d *(Cu(II))* and K_d *(M)* represent the distribution coefficient of Cu(II) and M ions, respectively. k_{IIP} and k_{NIP} represent the selectivity coefficient of Cu(II)-IIP and NIP, respectively.

3) Reusability of the Cu(II)-IIP

To test the reusability of the Cu(II)-IIP, five cycles of adsorption–desorption were tested. The Cu(II) was removed from the sorbent by washing with 2 mol·L^{-1} HCl and rinsed several times with DDW for neutralized pH. Then, dried under vacuum at 60 °C for 6 h before another cycle.

III. RESULTS AND DISCUSSION

A. Synthesis Strategy

Fig. 1 illustrates the main steps of the strategy involved in surface imprinting procedure. The synthesis of Cu(II)-IIP can be simply divided into three steps as follows: (1) vinyl groups were introduced to the surface of SBA-15 through chemical modification with MPS. (2) MAA immobilization on the decorated surface of SBA-15@MPS in the presence of Cu(II). In this step, surface imprinting was conducted and the shape memory polymer networks formed after the coordination between Cu(II) and the groups grafted on SBA-15. (3) removing chelated Cu(II) by 2 mol·L^{-1} HCl. The imprinted polymer which contained predetermined orientation and tailor-made cavities on surface of SBA-15 for Cu(II) was formed.

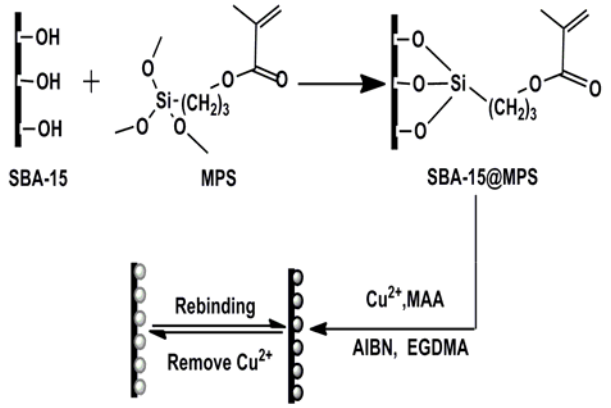

Fig. 1 Schematic illustration of preparation process of Cu(II)-IIP

B. Characterization

1) FT-IR analysis

Fig. 2 show the FT-IR spectra of SBA-15, SBA-15@MPS and Cu(II)-IIP. All of the samples displayed the stretching and bending vibration of Si–O–Si bond around 1084 cm^{-1}, 803 cm^{-1} and 462 cm^{-1}, suggesting that the structure of SBA-15 was well preserved after modification and polymerization. The peaks near 1635 cm^{-1} were attributed to stretching vibration of the surface Si-OH groups of SBA-15. The observed features around 3446 cm^{-1} indicate the stretching vibrations of –OH. After grafting of the vinyl groups, SBA-15@MPS exhibited the characteristic peaks of C=O bands at 1700 cm^{-1}. In addition, the vibration absorption bands of C–H bond near 2851 cm^{-1}, 2978 cm^{-1} also appeared. The results indicated that MPS was successfully introduced onto SBA-15. The Cu(II)-IIP exhibited obvious absorption bands around 1716 cm^{-1}, which was due to the C=O stretching vibration of carboxyl. All of the above results confirmed that Cu(II)-IIP was successfully synthesized.

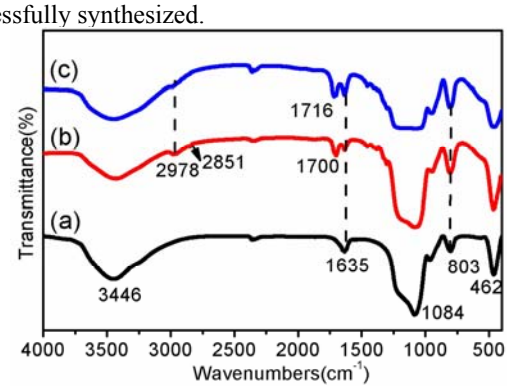

Fig. 2 FT-IR spectra of SBA-15(a), SBA-15-MPS(b), Cu(II)-IIP(c)

2) EDS analysis

The existence of Cu was further confirmed by the EDS analysis. In Fig. 3, the signal of oxygen and silica were the component of the SBA-15. The existence signal of carbon , which was due to the modification of MPS onto the surface of SBA-15. In addition, the signal of Cu was observed clearly in the sample of unleached Cu(II)-IIP (Fig. 3 a), and disappear after leached (Fig. 3 b). The above results support that Cu(II) ion has been successfully incorporated into the polymer, and it can be removed simply by washing with HCl aqueous solution.

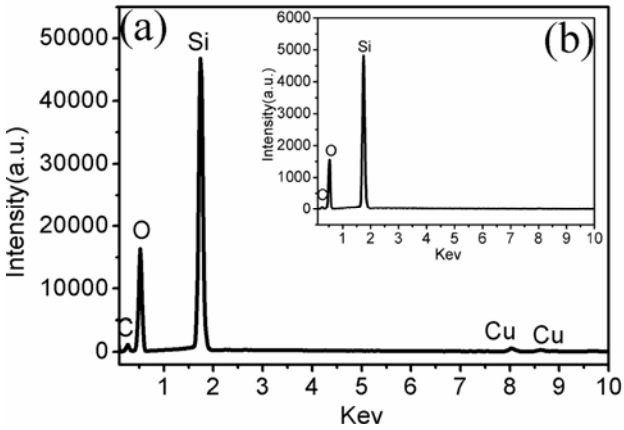

Fig. 3 EDS spectra of unleached Cu(II)-IIP(a) and leached Cu(II)-IIP(b)

3) XRD analysis

Powder XRD patterns results were showed in Fig. 4. Three XRD peaks at 0.85°, 1.50° and 1.72° were observed for Cu(II)-IIP, which corresponded to the (100), (110) and (200) reflections of SBA-15, respectively, suggesting that the structure of SBA-15 was well preserved. The decrease in the (100) XRD diffraction peak in Cu(II)-IIP provided evidence

that grafting mainly occurs inside the mesopore channels [30]. The result was further demonstrated by TEM.

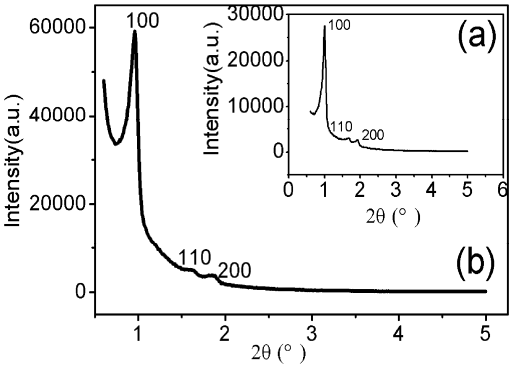

Fig.4 XRD patterns of SBA-15 (a) and Cu(II)-IIP (b)

4) Morphology analysis

The morphology and microstructure of SBA-15 and Cu(II)-IIP was analyzed by the SEM and TEM, respectively. The SEM images are presented in Fig. 5 (a) and (b). As can be seen, pure SBA-15 revealed short rod-like structures with relatively uniform size (Fig. 5 a). For the Cu(II)-IIP, the ordered morphology of SBA-15 was destroyed to a certain degree after a series of functionalization and the surface became rough since organic groups grafted on surface. Meanwhile, the TEM images were displayed in Fig. 5 (c) and (d). It can be clearly observed that channel-like structures running parallel to the longer direction, these channels displayed corresponded well to the typical structure of SBA-15. Compared with the two TEM images of SBA-15 and Cu(II)-IIP, we could conclude that the highly ordered mesoporous channels structure of the SBA-15 was well maintained and the pore size was decreased after functionalization. The results were consistent with BET analysis.

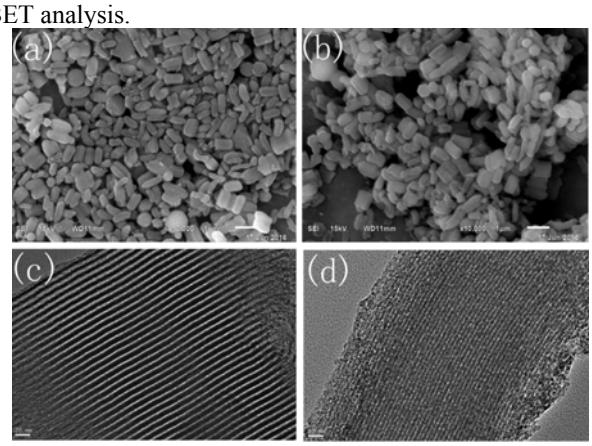

Fig.5 SEM images of SBA-15 (a) and Cu(II)-IIP (b), TEM images of SBA-15 (c) and Cu(II)-IIP (d).

5) BET analysis

The nitrogen adsorption–desorption isotherms of SBA-15 and Cu(I)-IIP are shown in Fig. 6. All samples exhibited typical type IV isotherms with clear hysteresis loops of H1 type associated with capillary condensation at P/P_0 from 0.6 to 0.8. Despite the decrease in the adsorbed amount of N_2 after polymerization in the surface of SBA-15, the shape of the hysteresis loops of Cu(II)-IIP remained the same. This also further indicated that the ordered hexagonal structure of SBA-15 was well preserved after modification.

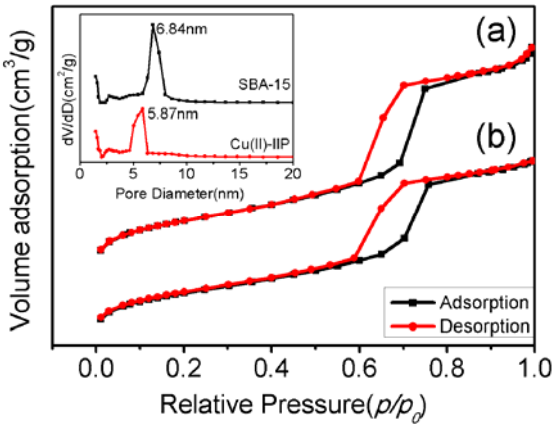

Fig.6. N_2 adsorption–desorption isotherms and pore size distribution (inset) of SBA-15 (a) and Cu(II)-IIP (b). The pore size distribution was calculated by the BJH method.

Table 1 summarizes the physical parameters of SBA-15 and Cu(II)-IIP that calculated from N_2 adsorption–desorption isotherms. Cu(II)-IIP shows a narrow pore size distribution centered at 5.87 nm, BET surface area was 375.22 $m^2 \cdot g^{-1}$ and its pore volume was 0.57 $cm^3 \cdot g^{-1}$, which showed a larger relative diminution, in comparison to its native SBA-15 counterpart (6.84 nm, 520.59 $m^2 \cdot g^{-1}$ and 0.75 $cm^3 \cdot g^{-1}$ for SBA-15). These changes were attributed to the incorporation of organic groups into the mesoporous framework.

TABLE I. PHYSICAL PARAMETERS OF SBA-15 AND Cu(II)-IIP MEASURED BY NITROGEN ADSORPTION-DESORPTION ISOTHERMS

Samples	BET surfaces area ($m^2 \cdot g^{-1}$)	Pore size (nm)	Pore volume ($cm^3 \cdot g^{-1}$)
SBA-15	520.59	6.84	0.75
Cu(II)-IIP	375.22	5.87	0.57

6) TG analysis

TG curves were employed to perform the thermal stability of Cu(II)-IIP. As can be seen in Fig. 7, all of the samples displayed a slight weight loss at temperatures from 40 °C to 200 °C, which was mainly due to the loss of absorbed water. As for Cu(II)-IIP, it can be obviously seen that the weight loss increased rapidly in the temperature ranging from 300 °C to 900 °C because of the thermal decomposition of the polymer (approximately 13.34%). The results also can demonstrated that the polymer was successfully grafted onto the surface of SBA-15.

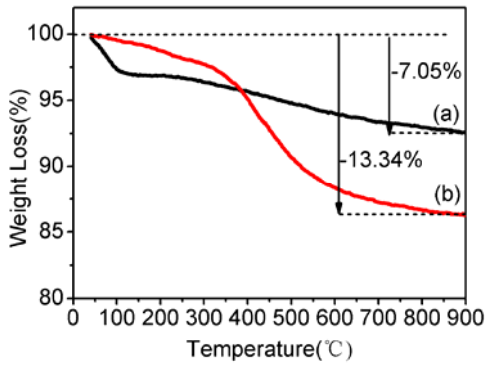

Fig. 7 TG curves of SBA-15 (a) and Cu(II)-IIP (b)

C. Adsorption Experiments

1) Effect of pH

pH is one of the most effective parameter for adsorption of metals on Cu(II)-IIP. The effect of pH values on Cu(II) ions adsorption was investigated at the range of 3–8, which is depicted in Fig. 8. The adsorption capacity of Cu(II) increased with an increasing in pH from 3 to 7, and then decreased slowly in pH from 7 to 8 and the maximum adsorption occurred around pH 7. It is explained that an excess of hydrogen ions have compete effectively with Cu(II) for bonding sites at acidic conditions, when the pH value was over 7, the hydrolyzation of copper ions maybe occurred, resulting in low adsorption capacity of Cu(II)-IIP. Therefore, 7 was selected to be the optimum pH for further work.

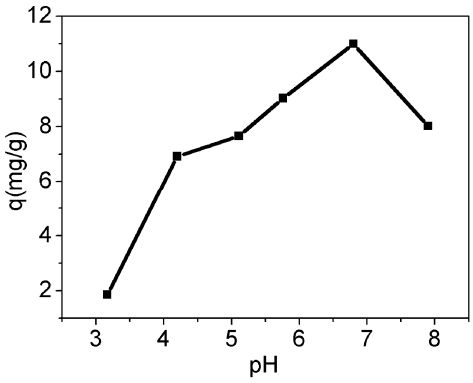

Fig.8 Effect of pH on adsorption of Cu(II) onto Cu(II)-IIP

2) Adsorption kinetics

The effect of contact time on adsorption of Cu(II) ions onto Cu(II)-IIP was shown in Fig. 9. The amount of Cu(II) ion adsorbed increases with time in the initial stage (0–40 min range), and then reach an equilibrium value in approximately 60 min. A further increase in contact time had a negligible effect on the amount of ion adsorption. According to these results, the equilibrium time was fixed at 1 h for the subsequent adsorption experiments to ensure that equilibrium was achieved.

The applicability of different kinetics models to the adsorption behavior was studied to make a better understanding of the adsorption mechanism. In this study, The equations of pseudo-first-order and pseudo-second-order shown as Eqs. (6) to (7) were employed to interpret the experimental data.

$$\ln(q_e - q_t) = \ln q_e - k_1 t \tag{6}$$

$$\frac{t}{q_t} = \frac{1}{k_2 q_e^2} + \frac{1}{q_e} t \tag{7}$$

where k_1 (min^{-1}) and k_2 ($g \cdot mg^{-1} \cdot min^{-1}$) are the rate constants of pseudo-first-order and pseudo-second-order model.

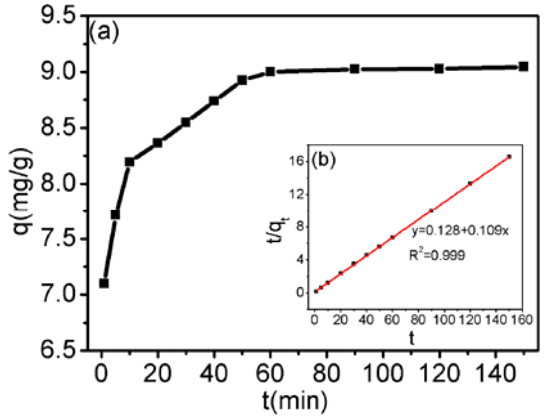

Fig.9 Effect of time on the adsorption of Cu(II) onto Cu(II)-IIP (a)and fitting data by pseudo-second-order model (inset) (b)

The rate constants of adsorption and linear regression correlation coefficients for Cu(II)-IIP were presented in Table 2 and fitted data by pseudo-second-order model displayed in Fig.9 (inset) , as can be clearly seen in the table, pseudo-second-order kinetic model well fit the adsorption of Cu(II) onto Cu(II)-IIP. Therefore, it is assumed that chemical process was the rate-limiting step in the adsorption process.

TABLE II. KINETIC PARAMETERS FOR Cu(II) ADSORPTION ON Cu(II)-IIP

Pseudo-first-order kinetics			Pseudo-second-order kinetics		
k_1(min^{-1})	q_{eq}($mg \cdot g^{-1}$)	R^2	k_2 ($g \cdot mg^{-1} \cdot min^{-1}$)	q_{eq}($mg \cdot g^{-1}$)	R^2
0.0565	1.85	0.931	0.093	9.17	0.999

3) Adsorption isotherm

The effect of initial ion concentration on Cu(II)-IIP and NIP was investigated at the rang from 10 to 800 $mg \cdot L^{-1}$. As can be seen from Fig.10. The adsorption capacity of Cu(II)-IIP for Cu(II) increased with increasing initial Cu(II) concentration in the aqueous solution. Compared with NIP, Cu(II)-IIP exhibited higher adsorption capacity at the corresponding concentration. The maximum adsorption capacity of Cu (II)-IIP was 25.03 $mg \cdot g^{-1}$ higher than that of

NIP at 25 °C.The results proved that the prepared adsorbents had more adsorption sites for the Cu (II) by using imprinting technology.

The adsorption isotherms were used to assess the binding properties in the batch rebinding method, which was a key for understanding the adsorption mechanism. Therefore, the adsorption properties were evaluated by adsorption isotherms in the batch experiments, which is shown in Fig.10. The equations of Langmuir and Freundlich isotherms shown as Eqs. (8) to (9).

$$\frac{C_e}{q_e} = \frac{1}{q_m k_L} + \frac{1}{q_m} C_e \tag{8}$$

Where k_L and q_m are the Langmuir coefficients, referring to the adsorption equilibrium constant and the maximum adsorption capacity, respectively.

$$\ln q_e = \ln K_F + \frac{1}{n} \ln C_e \tag{9}$$

where K_F is an indicative constant for the adsorption capacity and *1/n* is an empirical parameter.

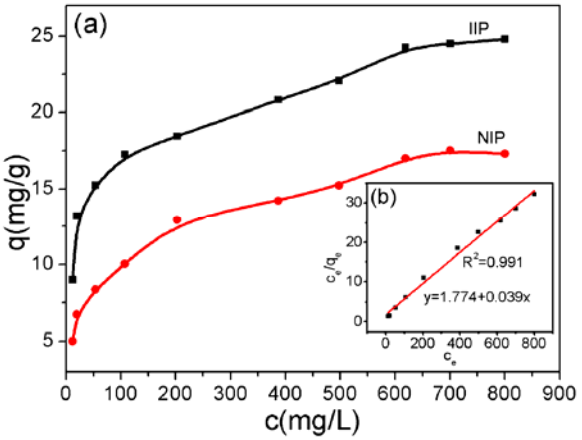

Fig. 10 Adsorption isotherms for adsorption of Cu(II) onto Cu(II)-IIP and NIP (a) and fitting data by Langmuir isotherms (b)

The isotherm parameters obtained from linear analysis of the two isotherm models were also presented in Table 3 and fitting data by Langmuir isotherms displayed in Fig.10 (inset). Data showed that the adsorption of Cu(II) on Cu(II)-IIP was well fitted to the Langmuir isotherm model.

TABLE III. THERMODYNAMIC PARAMETERS FOR ADSORPTION OF Cu(II) ONTO Cu(II)-IIP

Sorbent	Langmuir model			Freundlich model		
	q_m (mg·g^{-1})	k_L (mL·mg^{-1})	R^2	*1/n*	K_F (mg·g^{-1})	R^2
Cu(II)-IIP	25.64	0.022	0.991	0.207	6.283	0.942

4) Selectivity study

Competitive adsorption of the same charge or similar ionic radius ions from binary mixtures such as Cu(II)/Cd(II), Cu(II)/Fe(II), Cu(II)/Co(II), Cu(II)/Pb(II) were investigated by using Cu(II)-IIP and NIP, respectively. As can be seen in Table 4, the selectivity coefficient for Cu(II)/Cd(II), Cu(II)/Fe(II), Cu(II)/Co(II), Cu(II)/Pb(II) were 3.56, 2.32, 11.75, 4.73, respectively. Cu(II)-IIP exhibited an effective adsorption selectivity for Cu(II) in presence of competitive metal ions.

TABLE IV. DISTRIBUTION COEFFICIENT AND SELECTIVITY COEFFICIENT DATE OF Cu(II)-IIP AND NIP SORBENT

Metal ions	Cu(II)-IIP			NIP			
	q (mg·g^{-1})	K_d (L·g^{-1})	k_{IIP}	q (mg·g^{-1})	K_d (L·g^{-1})	k_{NIP}	k'
Cu(II)	13.59	108.80	3.56	13.71	109.27	3.23	1.10
Cd(II)	3.80	30.54		4.19	33.87		
Cu(II)	13.94	105.02	2.32	13.09	99.79	1.81	1.28
Fe(II)	6.52	45.30		7.80	55.07		
Cu(II)	11.91	86.99	11.75	13.90	104.96	8.79	1.34
Co(II)	1.13	7.40		1.80	11.94		
Cu(II)	15.50	123.02	4.73	13.33	104.21	3.82	1.24
Pb(II)	4.13	26.06		4.30	27.28		

5) Regeneration studies

In practical application, the potentiality to be reused is considered as an important factor to assess the value of an absorbent. The results of the regeneration studies were shown in Fig. 11, there was no significant decrease in adsorption capacity after a test of up to five adsorption–desorption cycles, demonstrating that the ion polymer is stable and reusable.

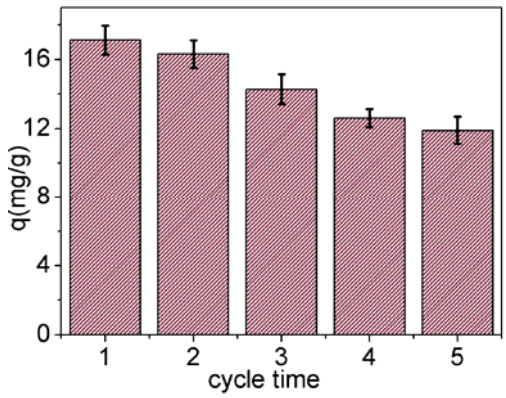

Fig. 11 Adsorption–desorption cycles of Cu(II)-IIP

IV. CONCLUSIONS

In this work, a new Cu(II) ion-imprinted polymer based on mesoporous SBA-15 functionalized with MPS was successfully synthesized by surface imprinting technique for selective removal of Cu(II) from aqueous solution. The imprinted polymer was characterized by FT-IR, EDS, XRD, TGA, SEM, TEM and N_2 adsorption–desorption. The adsorption capacity for Cu(II)-IIP was higher than that of NIP under the same conditions. Adsorption isotherm experiments indicated that the Langmuir model was well fitted isotherm model. The kinetics of adsorption followed

the pseudo-second-order model. Competitive adsorption studies illustrated that Cu(II)-IIP offered the advantages of selectivity toward Cu(II) in the presence of other metal ions. The prepared Cu(II)-IIP can be used more than five times without an obvious decrease in adsorption capacity, demonstrating that the Cu(II)-IIP supported on SBA-15 is stable and reusable.

ACKNOWLEDGEMENTS

The authors thank the support of the National Natural Science Foundation of China (No. 21266027 and No. U1507122).

REFERENCES

[1] Pereira FAR, Sousa KS, Cavalcanti GRS, et al. (2013) Chitosan-montmorillonite biocomposite as an adsorbent for copper (II) cations from aqueous solutions. Int. J.Biol. Macromol., 64:471-478.

[2] Debelius B, Forja J M, DelValls TA, et al. (2009) Toxicity of copper in natural marine picoplankton populations. Ecotoxicology, 18(8):1095-1103.

[3] Brown PA, Gill SA, Allen SJ (2000) Metal removal from wastewater using peat. Water Res. 34(16):3907-3916.

[4] He JS , Paul Chen J (2014) A comprehensive review on biosorption of heavy metals by algal biomass: Materials, performances, chemistry, and modeling simulation tools. Bioresour. Technol., 160:67-78.

[5] Stafiej A, Pyrzynska K (2007) Adsorption of heavy metal ions with carbon nanotubes, Sep. Purif. Technol., 58(1):49-52.

[6] Mauchauffée S, Meux E (2007) Use of sodium decanoate for selective precipitation of metals contained in industrial wastewater.Chemosphere 69(5):763-768.

[7] Verma VK, Tewari S, Rai JPN (2008) Ion exchange during heavy metal bio-sorptionfrom aqueous solution by dried biomass of macrophytes. Bioresour. Technol., 99(6):1932-1938.

[8] Kurniawan TA, Chan GYS, Lo WH, et al. (2006) Comparisons of low-cost adsorbents for treating wastewaters laden with heavy metals. Sci. Total Environ. 366(2-3):409-426.

[9] Chethan PD, Vishalakshi B (2013) Synthesis of ethylenediamine modified chitosan and evaluation for removal of divalent metal ions Carbohydr. Polym., 97(2):530-536.

[10] Alejandro GA, Virginia HM, Adrian BP (2011) Improving the adsorption of heavy metals from water using commercial carbons modified with egg shell wastes. Industrial and Engineering Chemistry Research,50(15):9354-9362.

[11] Yu JF, Wang YH, Fazle SH, et al. (2013) In situ synthesis of low silica X zeolite on ceramic honeycombs for adsorption of heavy metals. Journal of Porous Materials, 20(6):1525-1529.

[12] Ali S, Teruo HS, Tamao H, et al. (2011) Evaluating the adsorptive capacity of montmorillonitic and calcareous clays on the removal of several heavy metals in aqueous systems.Chemical Engineering Journal, 172(1):37-46.

[13] Kumar KY, Muralidhara HB, Nayaka YA, et al. (2013) Low-cost synthesis of metal oxide nanoparticles and their application in adsorption of commercial dye and heavy metal ion in aqueous solution. Powder Technology, 246:125-136.

[14] Lu YK, Yan XP (2004) An imprinted organic−inorganic hybrid sorbent for selective separation of cadmium from aqueous solution. Anal. Chem., 76(2):453-457.

[15] Xiang GQ, Wen SP, Jiang XM, et al. (2011) Determination of trace copper(II) in food samples by flame atomic absorption spectrometry after cloud point extraction. Iran.J.Chem.Chem.Eng. 30(3):101-107.

[16] Mendil D, Karatas M, Tuzen M (2015) Separation and preconcentration of Cu(II), Pb(II), Zn(II), Fe(III) and Cr(III) ions with coprecipitation method without carrier element and their determination in food and water samples. Food Chem. 177, 320-324.

[17] Nafiseh K, Farzaneh S (2016) A new magnetic ion-imprinted polymer as a highly selective sorbent for determination of cobalt in biological and environmental samples. Talanta, 146:244-252.

[18] Chen LG, Xu SF, Li JH (2011) Recent advances in molecular imprinting technology: current status, challenges and highlighted applications. Chem Soc Rev, 40(5):2922-2942.

[19] Fu JQ , Chen LG, Lia JH (2015) Current status and challenges of ion imprinting.J. Mater. Chem. A, 3:13598-13627.

[20] Tsoi YK, Ho YM, Leung KSY (2012) Selective recognition of arsenic by tailoring ion-imprinted polymer for ICP-MS quantification. Talanta, 89:162-168.

[21] Luo XB, Huang YN, Deng F (2012) A magnetic copper(II)-imprinted polymer for the selective enrichment of trace copper(II) ions in environmental water. Microchim Acta, 179(3):283-289.

[22] Ashkenani H, Ali Taher M (2012) Selective voltammetric determination of Cu(II) based on multiwalled carbon nanotube and nano-porous Cu-ion imprinted polymer. Journal of Electroanalytical Chemical, 683:80-87.

[23] Guo JJ, Su QD, Gan WE (2009) On-line Selective Solid-Phase Extraction of Copper with a Surface Ion Imprinted Silica Gel Sorbent. Journal of the Chinese Chemical Society, 56(4):763-770.

[24] Magner E (2013) Immobilisation of enzymes on mesoporous silicate materials. Chem.Soc. Rev. 42(15):6213-6222.

[25] Li JN, Qi T, Wang LN , et al. (2007) Synthesis and characterization of imidazole functionalized SBA-15 as an adsorbent of hexavalent chromium, Mater. Lett. 61(14-15):3197-3200.

[26] Meng XG , Liu Y, Meng MJ , et al. (2015) Synthesis of novel ion-imprinted polymers by two different RAFT polymerization strategies for the removal of Cs(I) from aqueous solutions, RSC, Adv.,5(17): 12517-12529.

[27] Liu Y, Qiu J, Liu ZC, et al. (2016) Tailor-made ion-imprinted polymer based on functionalized graphene oxide for the preconcentration and determination of trace copper in food samples. J. Sep. Sci. 39:1371-1378.

[28] Zhao DY, Feng JL, Huo QS, et al. (1998) Stucky, Triblock copolymer syntheses of mesoporous silica with periodic 50 to 300 angstrom pores. Science, 279(5350):548-552.

[29] Dai S, Burleigh MC, Shin YS, et al. (1999) Imprint coating: A novel synthesis of selective functionalized ordered mesoporous sorbents. Angew. Chem. Int. Ed. Engl., 38(9):1235-1239.

[30] Liu Y, Liu ZC, Gao J, et al. (2011) Selective adsorption behavior of Pb(II) by mesoporous silica SBA-15-supported Pb(II)-imprinted polymer based on surface molecularly imprinting technique. Journal of Hazardous Materials 186 (1):197-205.